Resolving the Gating Charge Movement Associated with Late Transitions in K Channel Activation

Andrey Loboda and Clay M. Armstrong
Department of Physiology, University of Pennsylvania School of Medicine, Philadelphia, Pennsylvania 19104 USA

ABSTRACT We examined the late transitions in the activation sequence of potassium channels by analyzing gating currents of mutant *Shaker* IR channels and using the potassium channel blocker 4-aminopyridine (4AP). Gating currents were recorded from a double mutant of *Shaker* that was nonconducting (W434F mutation) and had the late gating transitions shifted to the right on the voltage axis (L382C mutation), thus separating the late transitions from the early ones. 4AP applied to the double mutant blocked the final transition and made possible novel observations of the isolated intermediate transitions, the ones that immediately precede the final opening of the channel. These transitions, which have not been well characterized previously, produce a distinct fast component in the gating current tails. Two intermediate transitions contribute to the fast component and carry 23% of the total gating charge. The effect of 4AP is well modeled as a selective block of the final gating transition, which opens the channel. The final transition contributes ~5% of the total gating charge.

INTRODUCTION

Potassium channels consist of four identical subunits (MacKinnon, 1991) with six transmembrane segments in each. The activation of a K channel requires a sequence of conformational changes that are driven by depolarization. The voltage-sensing element is the S4 transmembrane segment, containing in *Shaker* seven positively charged amino acids. The S4 moves in response to a voltage change and forces the opening of an internally located gate. The steep voltage dependence of channel activation suggests that the equivalent of several electron charges cross the membrane in each subunit during activation. This charge movement generates detectable gating current (Armstrong and Bezanilla, 1973), which can be used for studying events in the closed channel. The total gating charge is estimated to be ~13 e_0 (Schoppa et al., 1992; Aggarwal and MacKinnon, 1996; Seoh et al., 1996).

Much work has been devoted to determining the number of states in the activation process, the kinetics of the transitions among the states, and the significance of these states and transition rates in terms of the structure of the K channel protein (Tempel et al., 1987; Stühmer et al., 1991; Schoppa et al., 1992; Tytgat and Hess, 1992; Bezanilla et al., 1994; Hoshi et al., 1994; Zagotta et al., 1994a,b; Schoppa and Sigworth, 1998a,b,c; Ledwell and Aldrich, 1999). These studies have used measurements of macroscopic and single-channel ionic current, and gating current, or all three together, on wild-type and mutant K channels. Many of these studies have divided the activation sequence into early steps followed by later ones that are qualitatively different and easily distinguishable kinetically. Two fundamental observations supporting this separation are derived from gating current tails recorded as the channels return to rest after partial or complete activation. Following partial activation, the tails are fast, but they become very slow and have a distinct rising phase after a depolarization large and long enough to fully activate the channels (Bezanilla et al., 1991, 1994; Stefani et al., 1994; Zagotta et al., 1994a). This observation shows clearly that a transition late or last in the activation sequence is very slowly reversible in comparison with the earlier steps. The second observation comes from study of mutations involving the leucine residue at position 382 in *Shaker*. Changing this residue to a valine does not affect the early steps of activation, as judged from the gating current, but shifts late transitions far to the right on the voltage axis, effectively separating them from the early steps (Schoppa et al., 1992). The clear distinction in properties between early and late steps has led to the idea that the early ones may involve events within the individual subunits, whereas the late steps may be concerted, involving simultaneous action in all subunits.

The primary effect of the L382V mutation is attributed to dramatically faster backward rate constants of the late transitions, especially the penultimate step. As a consequence, a much larger voltage is required to make the equilibrium of these steps favorable to channel opening. The fast reverse rate constants of these steps make the gating current tails of L382V much faster than for the wild-type channels. Specifically, Schoppa and Sigworth (1998c) postulate that the activation sequence consists of 1) three transitions in each of the four subunits, during which the subunits change independently of each other, followed by 2) two transitions in which the subunits change in concert. Charge movement during the early transitions is ~9e, and the two concerted transitions are responsible for 2 e_0, of which 0.7 e_0 is in the final transition.

The K channel blocker 4-aminopyridine (4AP), which is a major tool in the present study, blocks potassium current in a relatively complicated manner that has been interpreted

Received for publication 23 January 2001 and in final form 23 April 2001.
Address reprint requests to Dr. Clay M. Armstrong, Department of Physiology, University of Pennsylvania School of Medicine, B-701 Richards Building, Philadelphia, PA 19104-6085. Tel.: 215-898-7816; Fax: 215-573-5851; E-mail: carmstro@mail.med.upenn.edu.
© 2001 by the Biophysical Society
0006-3495/01/08/905/12 $2.00

mechanistically in more than one way (Kirsch et al., 1986; McCormack et al., 1994). 4AP blocks a small fraction of the total gating charge involved in the activation gating of *Shaker* (McCormack et al., 1994).

In this paper we compare the effect of 4AP on the activation gating of two *Shaker* IR mutants: the nonconducting W434F mutant (this will be called NC), and a double mutant, W434F + L382C, to be called NC-L2C. Combining 4AP to block the last step with the NC-L2C mutation, which separates the early (independent) steps from the late steps, we have isolated and characterized the gating steps that immediately precede the final opening of the channel. We find that the effect of 4AP can be explained by a selective block of the last (concerted) step in the activation sequence. A model for 4AP action is presented in the next paper.

MATERIALS AND METHODS

The NC mutation of *Shaker* had the following base characteristics: inactivation was removed (Δ6–46; Hoshi et al., 1990), and the channels were rendered nonconducting by the W434F mutation (Perozo et al., 1993). W434F has the advantage that K^+ can be retained in the medium, which is essential because it has been shown that gating current changes drastically in the absence of K^+ (Melishchuk et al., 1998). The other mutant used, NC-L2C, added L382C to the base channel, thus altering the voltage dependence of the late steps in channel activation.

Mutagenesis and expression

Using polymerase chain reaction, mutations were engineered in *Shaker* IR, the *Shaker* H4 K^+ channel with the Δ6–46 mutation that removes N-type inactivation (Hoshi et al., 1990). For expression, the channel cDNA was subcloned into the GW1-CMV expression vector (British Biotechnology, Oxford, UK). The mutants were transiently expressed heterologously in tsA201 cells (HEK 293 cells, ATCC CRL 1537, stably transfected with SV40 large T antigen). The channel plasmid (10 μg) was co-transfected with the πH3-CD8 plasmid. Cells expressing the CD8 antigen were identified visually by antibody-coated beads. Cells were transfected by electroporation as described previously (Jurman et al., 1994).

Electrophysiology

Ionic and gating currents were recorded in whole-cell configuration 27–72 h after transfection. Membrane potential was controlled using custom-made software and hardware operated through an IBM PS-2 computer. Currents were recorded using glass pipettes prepared from Kimax-51 capillary tubes (Kimble). The standard extracellular solutions (named 140Na or 140Na 10K) used for these experiments contained (in mM) 140 NaCl, 0 or 10 KCl, 6 $CaCl_2$, 10 HEPES (NaOH), pH 7.4. The intracellular (pipette) solutions were N-methylglucamine (NMG), 140 NMG chloride; K, 140KCl; and NMG 15K, 125 NMG chloride, 15KCl. All intracellular solutions also contained 10 HEPES and were adjusted to pH 7.4 with *N*-methylglucamine. Solutions will be referred to as external//internal, e.g., 140Na 0 K//140 K. Currents were filtered at 10 KHz and sampled at 20, 50, or 100 kHz. Electrode resistance was in the range of 1–2 MOhm. Capacitive currents and leak were subtracted online using a control pulse in the −140-mV to −190-mV voltage range to generate the transient used for subtraction. The experiments were done at room temperature (20–22°C).

RESULTS

The effect of 4AP can be explained by selective inhibition of the final transition

The major features of activation and deactivation gating in the NC channel are shown in Fig. 1 *A* (cf. Perozo et al., 1993). Beginning with activation, I_g ON has a quick rise and simple decay kinetics after a small depolarization (traces 1 and 2). Following a depolarization large enough to fully activate most channels (trace 3), the rise of I_g ON is somewhat slower, and the decay kinetics are complex and prolonged as the channels move through the numerous states of the activation sequence. For the largest depolarization (trace 4), transit through these states is rapid, and I_g ON is large and brief.

Turning to the deactivation tails seen on repolarization, in trace 1 the tail jumps in amplitude too quickly to resolve, and the decay of the tail current (at −140 mV) is quick and monotonic. These are the characteristics of the backward transitions that return channels from partially activated back to the resting state. In trace 2 there is a similar fast component, followed by a slow component that represents slow deactivation of a small number of fully activated channels; the return transition from the fully activated state is slow. With depolarizations that are large enough to fully open conducting *Shaker* channels (traces 3 and 4) the fast component is absent, and there is only a slow component with a pronounced rising phase; all of the channels have reached the fully activated state from which return is slow.

Addition of 1 mM 4AP, a saturating concentration in W434F, has little effect on I_g as channels activate (I_g ON), indicating that most of the transitions occur almost normally. In contrast, effects on tail gating currents are dramatic after large depolarizations (cf. McCormack et al., 1994). The initial amplitudes of the tails in traces 3 and 4 are very large compared with traces 3 and 4 from Fig. 1 *A*. They have no resolvable rising phase, and decay kinetics are quick. Finally, unlike NC channels in the absence of 4AP, decay kinetics do not change with the size of the depolarization. 4AP does not affect I_g ON or OFF elicited by small steps (traces 1 and 2), showing that neither the forward nor the backward rates of the early transitions are altered. This pattern can be summarized and explained by saying that 4AP strongly hinders the slowly reversible final transition in the activation sequence.

The L382C mutation (Holmgren et al., 1996), like the extensively studied L382V (Schoppa and Sigworth, 1998b), shifts the opening of channels to more depolarized potentials (cf. Fig. 6 *D*) and modifies gating currents. I_g ON of the NC-L2C channel decays as a single exponential and lacks the slow component at intermediate depolarizations that is seen with the NC channel (Fig. 1 *C*). I_g OFF for NC-L2C after progressively larger depolarizations has an initial jump rather than a rising phase, and decays rapidly.

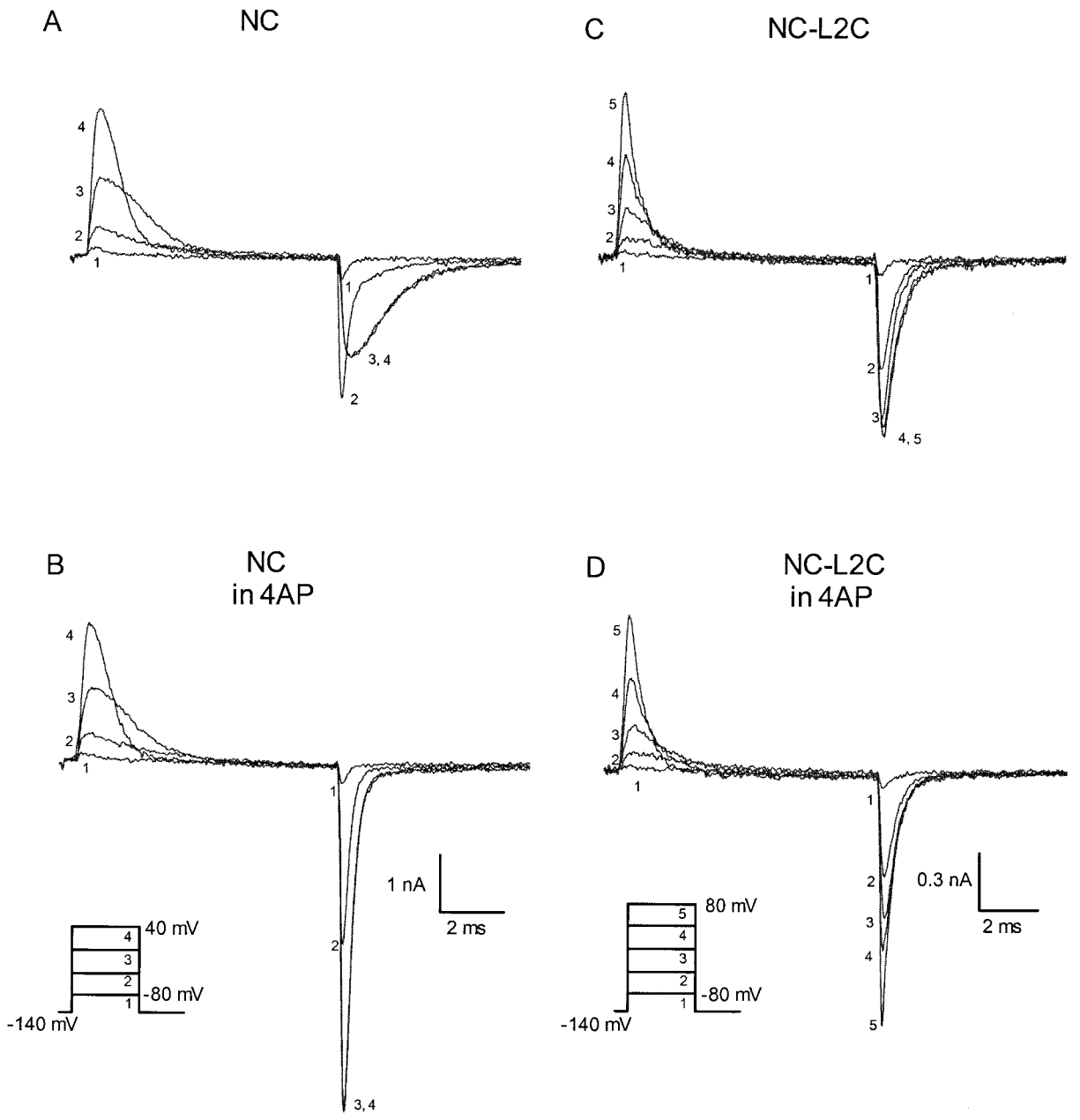

FIGURE 1 The effects of 4AP and the L382C mutation on I_g of nonconducting W434F *Shaker* B potassium channel. (*A*) I_g of the NC channel (W434F *Shaker* IR) were elicited by depolarizing pulses to test voltages between −80 and 40 mV in 40-mV increments (holding potential, −140 mV). (*B*) I_g of the NC channels in the presence of 1 mM 4AP. Recordings were made in the same cell and using the same protocol as in *A*. (*C*) I_g of the NC-L2C channel (the double mutant L382C + W434F) were induced by voltage steps to −80 through 80 mV in 40-mV increments (holding potential, −140 mV). (*D*) I_g of the NC-L2C channel in the presence of 1 mM 4AP; same cell and protocols as in *C*. Solutions, NMG//NMG 15K.

Our relatively high-resolution records make clear that 4AP alters the tail gating currents of NC-L2C after fully activating depolarizations (cf. McCormack et al., 1994, where such an alteration is not seen). Tails in traces 4 and 5 are faster and have larger amplitude than the respective traces without 4AP. This detail turns out to be important in resolving the mechanism of 4AP action as discussed below. There are no significant changes in I_g ON, showing that in NC-L2C, as in NC, most of the activation transitions are unaffected by 4AP. Tail gating currents after depolarizations up to 0 mV (sufficient to drive the early but not the late transitions in NC-L2C) are not altered by 4AP (traces 1–3 in Fig. 1 *D*).

The gating charge-voltage (*Q-V*) curve (Fig. 2) provides complementary information about the effects of 4AP and the L382C mutation. As shown by the white bars in the chart, there is no detectable effect of 4AP on the NC channel negative to

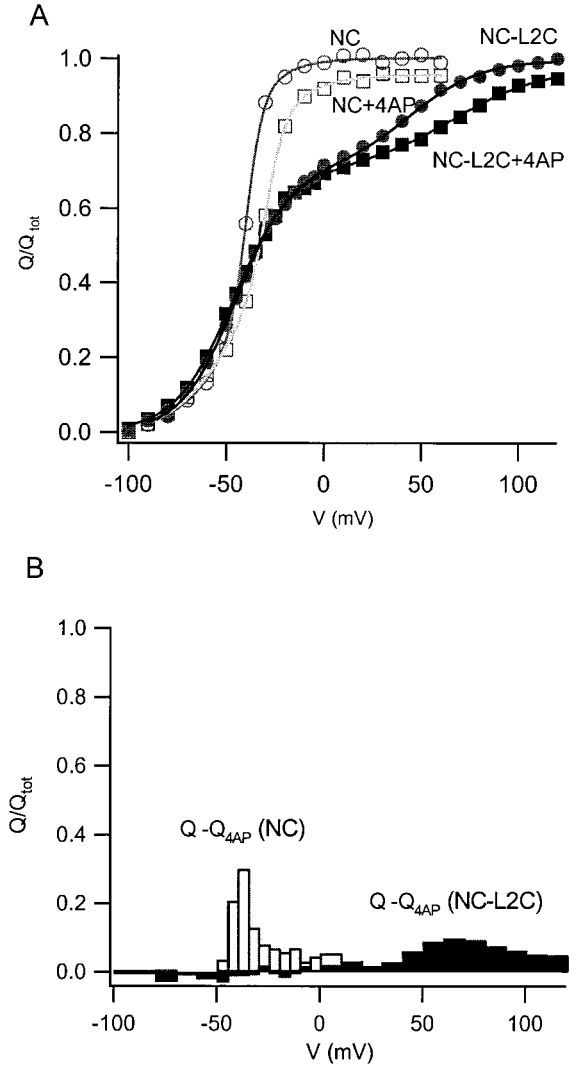

FIGURE 2 Changes in the *QV* curve caused by 4AP and the L382C mutation. (*A*) Gating charge was measured as the area under I_g OFF after a depolarization to a test voltage. The plots are normalized relative to the maximal value of the gating current Q_{tot}. 4AP blocks ~5% of the total gating charge in both NC and NC-L2C channels at high V_m. (*B*) The amount of charge blocked by 4AP as a function of voltage is given by the white bars for NC and by the black bars for NC-L2C. The amount of blocked charge was obtained by subtracting the *QV* curve in the presence of 4AP from the QV with no 4AP. Solutions, NMG//NMG 15K.

−50 mV. Near −40 mV, where conduction-capable *Shaker* channels just begin to open, 4AP prevents a substantial proportion of charge movement (up to 30%). Finally, above −10 mV, where the majority of channels populate the last closed state, 4AP reduces total gating charge by ~5%. The missing charge above −10 mV is the charge associated with the final transition, which is blocked by 4AP.

The *Q-V* curve of the NC-L2C channel (closed circles) separates visually into two components: 1) a Boltzmann-like left part, which starts to rise around −80 mV, has a half-voltage around −40 mV, and approaches saturation near 0 mV and 2) *A* slowly rising right part, in the 0–100-mV range, which contains about a third of total gating charge. Part 1 corresponds to the early transitions in the activation scheme. It is similar but not identical to its counterpart in the NC channel, because early transitions are only slightly affected by L382C. Transitions near the open state, which carry about a third of total gating charge, contribute to the slowly rising part of the curve at positive potentials. When 4AP is added, the gating charge moved between −80 mV and 0 mV is unchanged, again showing clearly that 4AP does not affect the early transitions. At ~0 mV the curves with and without 4AP diverge significantly, but then again come closer together at +80 to +100 mV. This is made clear by the black bars of the chart in the lower panel. About 12% of the total charge is blocked at +70 mV, declining to 5% at +100 mV. It is worth noting that at high voltage ~5% of the total gating charge is blocked by 4AP in both kinds of channels (NC and NC-L2C).

The results obtained in Figs. 1 and 2 are compatible with the model of Schoppa and Sigworth (1998c) in which the activation sequence consists of 1) early steps, which carry about two-thirds of the gating charge; 2) the final opening (or first closing) transition, which is blocked by 4AP; and 3) the intermediate steps (thought to be concerted), which occur between the early transitions and the final opening transition. Scheme SSs gives a simplified version of the model that we used for ease of computation, and because we were not concerned with early events in the activation sequence:

$$\underbrace{C_1 \leftrightarrow \cdots \leftrightarrow C_k}_{\text{early steps}} \leftrightarrow \underbrace{C_{n-1}}_{\text{intermediate}} \leftrightarrow \underbrace{C_n \leftrightarrow O}_{\text{final}} \qquad \text{(Scheme SSs)}$$

The L382C mutation changes the shape of the *Q-V* curve, but not the total amount of charge, by shifting the mid-voltage of the intermediate and final transitions to the right on the voltage axis (cf. Schoppa et al., 1992; Schoppa and Sigworth, 1998b). Given that 4AP reduces the total gating charge by only 5%, it seems likely that it blocks only the final transition. This block makes I_g OFF after large depolarizations faster in both the NC and NC-L2C channels (Fig. 1, *B* compared with *A* and *D* compared with *C*).

Isolating the intermediate transitions using NC-L2C channels and 4AP

The L382C mutation shifts the late transitions to more positive voltages, effectively separating them from the early ones. Thus, by using NC-L2C together with 4AP to block the final transition, only the intermediate transitions occur above 0 mV; the early transitions are completed at or below 0 mV. This isolation procedure is employed in many of the following figures.

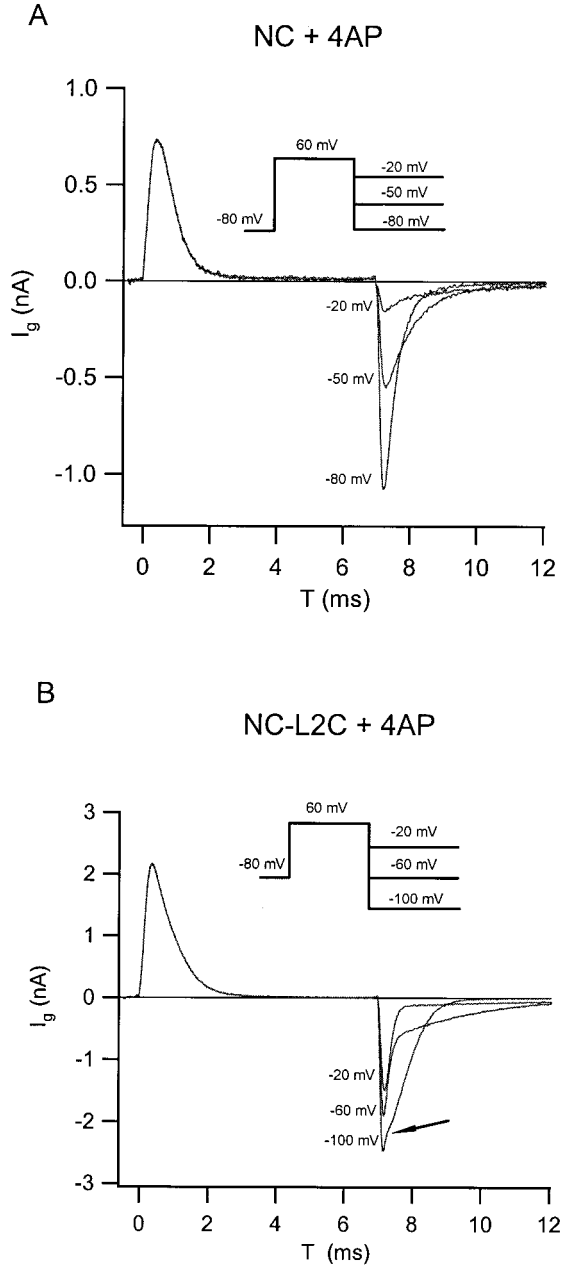

FIGURE 3 A fast component is present in I_g OFF of the 4AP-treated NC-L2C channel but not in the NC channel. (*A*) I_g OFF of 4AP-treated NC channels can be fitted with a single exponential at any repolarizing potential. (*B*) In contrast to the NC channel, I_g OFF of the NC-L2C channel consists of two kinetically distinguishable components. At −20 mV only the fast component is present. Solutions, NMG//NMG 15K.

Isolation of the intermediate transition in tail currents by this procedure is illustrated in Fig. 3. The tail current of the NC channel in 4AP (Fig. 3 *A*) is a single exponential to a good approximation for all repolarization voltages. For the NC-L2C channels the tails in 4AP have two kinetic components after depolarizations large enough to fully activate the channels. The fast component in these tails is generated by the intermediate transitions, and the slow one is associated with the early steps (see diagram above). At −20 mV the slow component is quite small, and its amplitude changes little by trace end due to the slowness of the transitions among the early states. At −60 mV both components are clearly visible, and the slow one decays visibly during the trace. Finally, at −100 mV the slow component is dramatically faster but distinguishable from the fast one by a notch (arrow).

The fast component generated by the isolated intermediate transitions can also be seen in the absence of 4AP

In the (conducting) L2C channel without 4AP the fast tail component representing the intermediate transitions (Fig. 4 *A*) first appears after a short activating step (arrow). At this time the intermediate states are partially populated, but few channels have progressed to the open state. The fast component reaches its maximum with a slightly longer step, just as the channels are opening. When the channels are almost fully open (3-ms step) the fast component has decayed to near zero, because almost all channels have migrated to the open state. The reverse (closing) transition from the open state is slow, even in L2C; once the channels pass into the open state, this slow reverse step limits the otherwise fast charge movement that arises from the intermediate transitions.

Upon application of 4AP (Fig. 4 *B*), the ionic current is abolished due to selective block of the final transition (see Figs. 1 and 2). The block of the final step eliminates both the decay of the fast component and the emergence of the slow component; the channels do not transit into the open state and are not retarded on repolarization by the slow, rate-limiting step out of the open state. This figure provides perhaps the clearest graphic summary of 4AP action.

I_g generated by the isolated intermediate transitions is also seen with NC-L2C channels (Fig. 4, *C* and *D*). In the absence of 4AP the fast component is present in the tails only transiently as channels pass through the intermediate states and into the fully activated state. As judged from the decay of the fast component, both conducting and nonconducting mutants undergo a gate-opening transition with about the same speed. Application of 4AP to the NC-L2C channel blocks the final opening transition and thus prevents the decay in the fast component (Fig. 4 *D*), as was also seen with L2C.

There are two intermediate transitions

Isolation of the intermediate transitions makes possible for the first time the characterization of their properties. The first question is how many transitions are represented in the fast component. To determine this, we selectively exercised

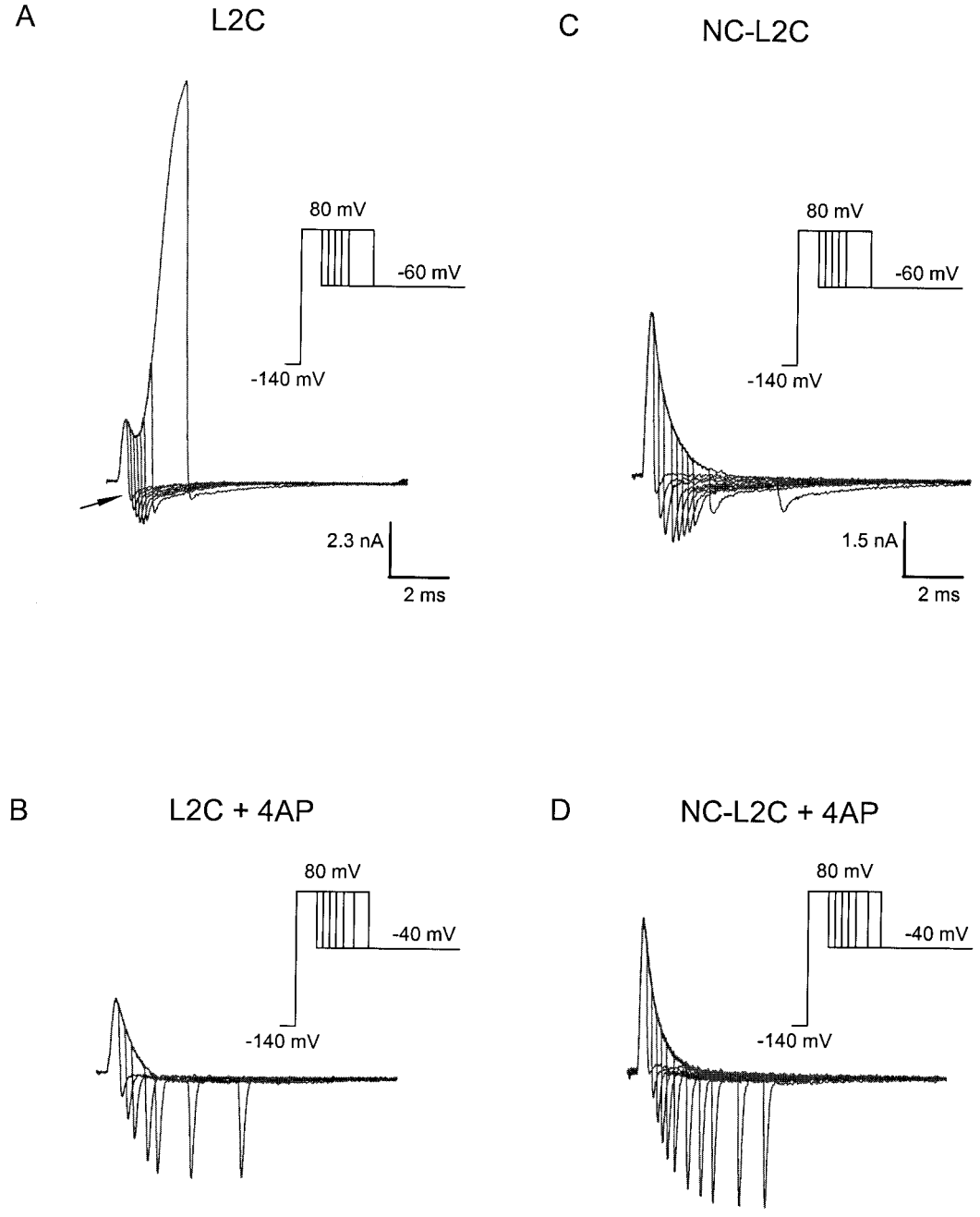

FIGURE 4 The time course of the fast component as a function of the pulse duration with and without 4AP. (*A*) A family of I_K and I_g traces was elicited by depolarizations to 100 mV for different durations. In the step to 80 mV, I_g ON is followed by I_K, which develops after I_g ON has peaked. I_g tails at −60 mV after a pulse to 100 mV have a fast component, followed by a slow one. The fast component is transient and best seen as channels begin to open. It becomes much smaller as depolarization lengthens. The decay in the amplitude of the fast component coincides with the activation of the ionic current. Solutions, NMG//140K. (*B*) 4AP at 1 mM blocks the ionic current and prevents the decay in the amplitude of the fast component. The fast component is larger than in *A* because the channels are prevented from entering the fully activated state from which return is slow. Solutions, NMG + 4AP//140K. (*C* and *D*). A fast component with analogous properties is seen in the tail currents of the NC-L2C channel. Solutions, NMG//NMG 15K.

these transitions in NC-L2C with the protocols shown in Fig. 5. V_m in part Fig. 5 *A* is initially pulsed to 100 mV, putting most channels in state C_n, the rightmost closed state (4AP prevents the final transition to state O). A 5-ms pulse to 0 mV elicits the gating current seen as the fast component in previous figures, generated as the channels move to state C_k in the scheme above. Because V_m does not go negative to 0 mV, the channels go only as far as state C_k. Subsequent pulses to 30, 60, or 90 mV (Fig. 5 *A*) resulted in outward gating current, generated by rightward movement from C_k

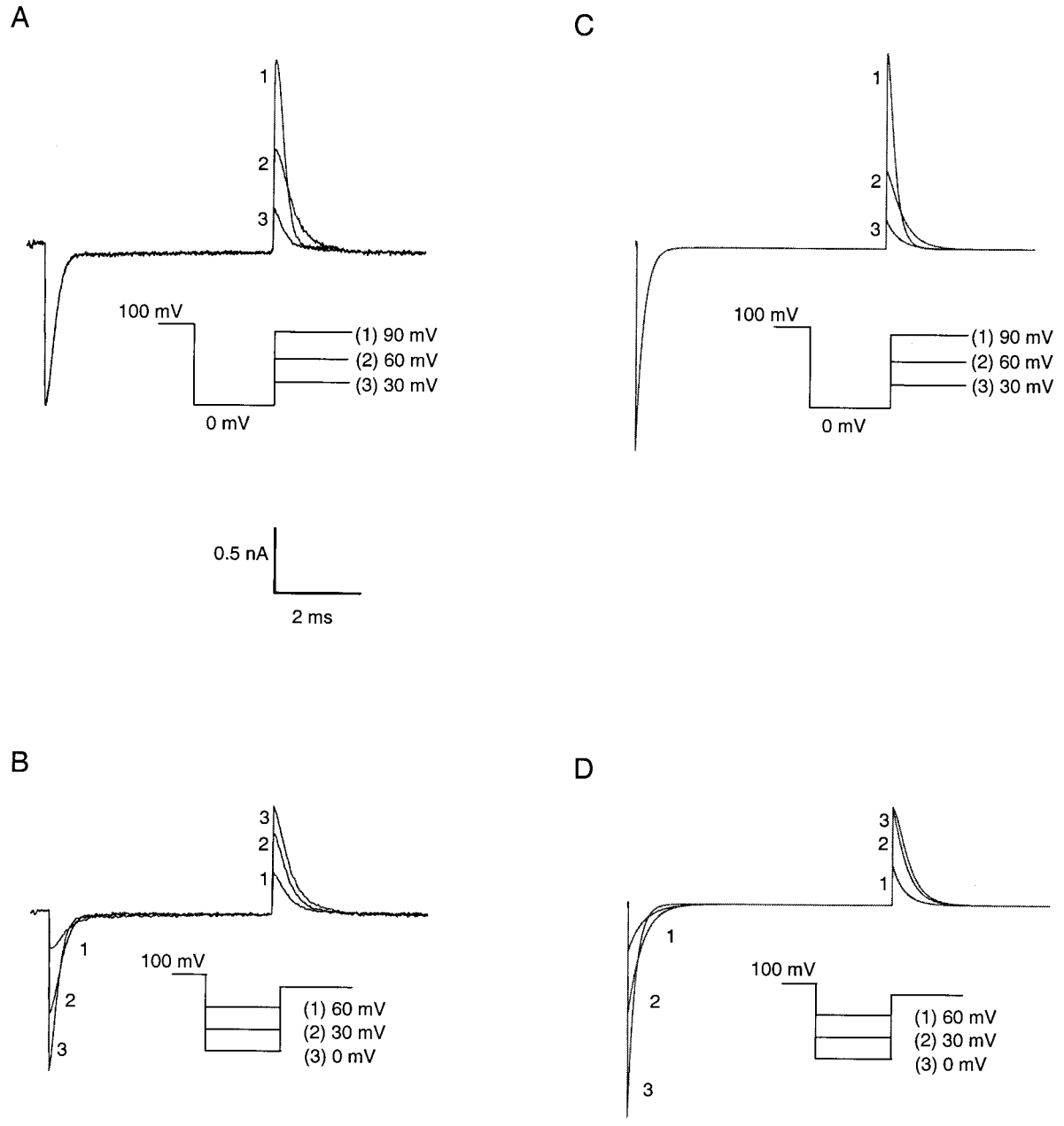

FIGURE 5 Kinetics and voltage dependence of the fast component. The fast component of I_g was measured in isolation from the NC-L2C channel in the presence of 4AP. (*A*) Forward rates of the intermediate transitions generating the fast component seen in Fig. 4 were studied. The membrane was first depolarized from a holding potential of −140 mV to 100 mV to move all channels to the rightmost closed state (4AP prevented the final transition), repolarized to 0 mV, and then depolarized again to 30, 60, or 90 mV. (*B*) The backward rates for the same transitions were examined. After a depolarization to 100 mV from the holding potential −140 mV, the membrane was repolarized to 0, 30, and 60 mV, followed by a depolarization to 100 mV. (*C* and *D*) Simulations of the gating currents produced by the intermediate transitions from Scheme 2 (see Discussion) provide a good fit to the records of the fast component. *C* and *D* simulate *A* and *B*, respectively. Solutions, NMG//NMG 15K.

into the intermediate states. These currents become larger with voltage as more channels move further to the right among the intermediate states, and they show characteristic changes in their kinetics, which are modeled in Fig. 5 *C*. Leftward movement from state C_n into other intermediate states was examined in Fig. 5 *B*, where the membrane was repolarized from 100 mV to 0, 30, or 60 mV. Finally, just before the last step (Fig. 5 *B*), the channels are distributed among the intermediate states as determined by V_m, and move to state C_n after stepping to 100 mV. These results are used in Fig. 5 *D* to constrain the properties of the intermediate steps in the gating scheme (see Discussion).

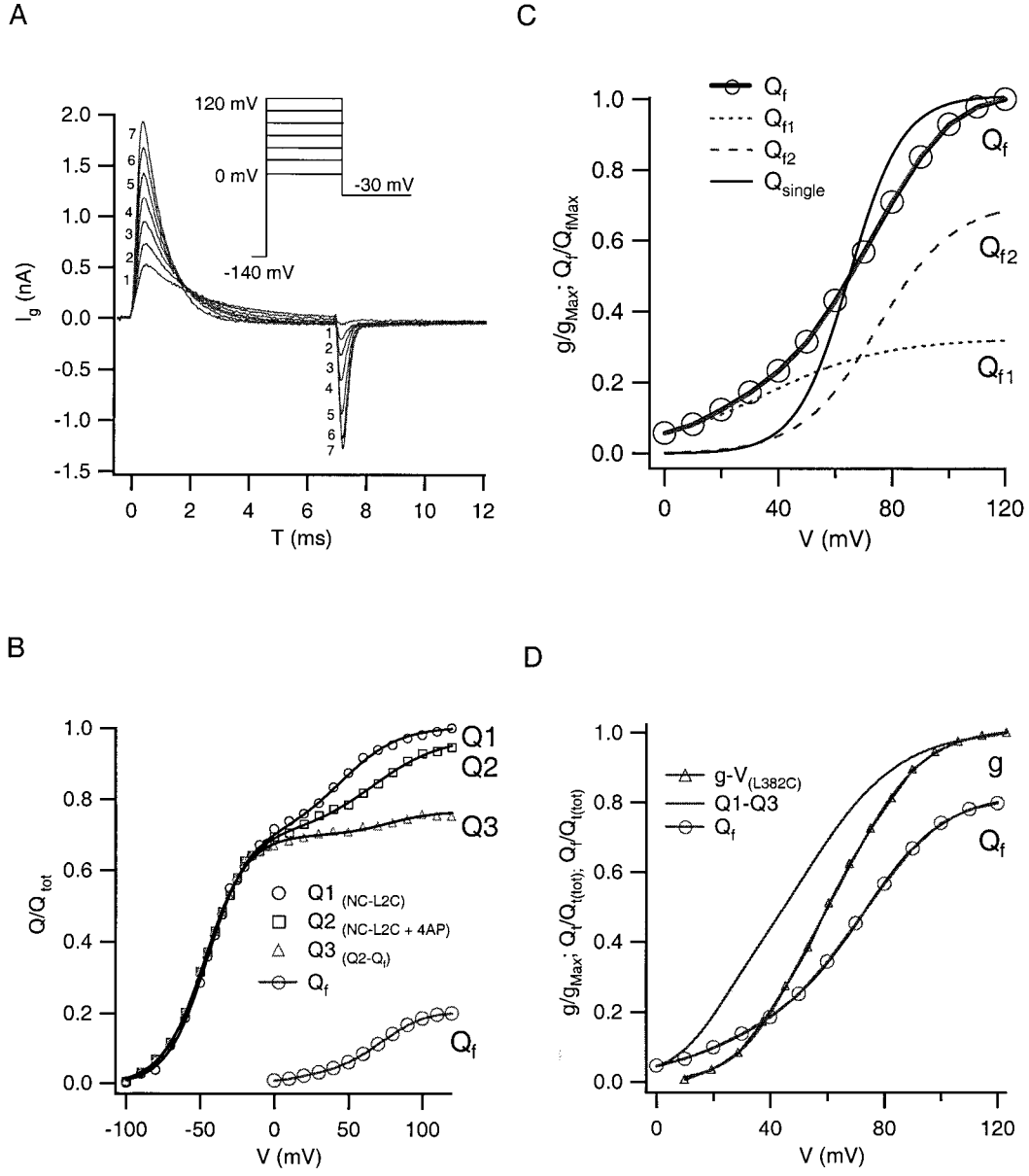

FIGURE 6 Voltage dependence of the gating transitions that generate the fast component. (*A*) I_g ON and OFF are shown for depolarizations from −140 mV to the indicated voltages with return to −30 mV. Gating charge of the fast component (plotted as Q_f in *B*) was measured as the area under the I_g OFF spike, using NC-L2C in 1 mM 4AP. At −30 mV the fast component is seen in almost perfect isolation. (*B*) Three *QV* curves are plotted in addition to Q_f from *A*. *Q*1, the gating charge for all transitions of the NC-L2C channels in no 4AP (see Fig. 2); *Q*2, the gating charge for all transitions of the NC-L2C channel in 1 mM 4AP (see Fig. 2); *Q*3, the difference between *Q*2 and Q_f; *Q*3 is the charge movement generated by the early transitions. (*C*) The *QV* curve of the fast component (Q_f) cannot be fit with a single Boltzmann curve (Q_{single}). Two transitions, Q_{f1} and Q_{f2} are required to account for the charge (23% of the total gating charge) and steepness of the Q_f curve. Their sum is given by the circles, which superimpose on the Q_f curve. (*D*) The gating charge of the intermediate steps as a function of V_m is given by Q_f. Q_1–Q_3, the gating charge of the late (intermediate + final) transitions was obtained by subtracting the gating charge of the early transitions (*Q*3 in *B*) from the *QV* curve of the NC-L2C channel (*Q*1 in *B*). The *g-V* curve of the conducting L2C mutant shows the percentage of channels that reach the open state at given potentials. All three curves are normalized. Q_1–Q_3 lies to the left of Q_f because of the sucking action of the forward bias of the final transition. This sucking action is present in Q_1–Q_3 but absent in the Q_f curve because 4AP blocks the final transition. Solutions, NMG//NMG 15K.

The protocol and sample records used to determine the gating charge in the intermediate steps are shown Fig. 6 *A*. At the end of an activating pulse to 120 mV, the channels (in 4AP) are all in state C_n. A step back to −30 mV pushed the channels to the left in the gating sequence, completely through the intermediate states. Contributions to the current from the early transitions could be easily separated out because of their slowness at −30 mV. The net charge for

transitions among the intermediate states as a function of V_m is given by the lowest curve, Q_f, in Fig. 6 *B*. Q_1 and Q_2 (from Fig. 2) show, respectively, the total gating charge in the NC-L2C channel without and with blockade of the final transition by 4AP. $Q3$ was obtained by subtracting Q_f from $Q2$ and in theory gives the Q-V of the early transitions, i.e., the Q-V stripped of both the intermediate transitions (subtracted out) and the final transition (blocked by 4AP). These transitions are largely complete at 0 mV.

Fig. 6 *B* also shows the fraction of the total gating charge that is associated with the early, intermediate, and final transitions. Measured at 120 mV, $Q1$ is the total moveable gating charge. The difference between $Q1$ and $Q2$ at 120 mV represents the gating charge of the final transition, and is ~5% of the total. This is the charge movement blocked by 4AP. The intermediate transitions, as given by Q_f, carry ~23% of the total gating charge ($Q2$–$Q3$ at 120 mV). The early steps, curve $Q3$ at 120 mV, account for the other two-thirds of the gating charge. Taking the total gating charge as ~13 e_0 (Schoppa et al., 1992; Seoh et al., 1996), the intermediate transitions would carry ~2.9 e_0, and the final transition would carry 0.65 e_0.

The Q-V curve of the fast component (Fig. 6 *C*) shows that a single transition cannot account for the observed gating charge movement. As noted, the fast component carries 23% of the total gating charge, or ~2.9 e_0. A single transition with this charge (Q_{single} in Fig. 6 *C*) fits the data very poorly. Thus, at least two transitions are required for a reasonable fit. These transitions were sufficiently separated in voltage range that they could be approximated by two Boltzmann curves carrying Q_{f1} ($V_{1/2}$ = 34 mV, q = 1.1 e_0) and Q_{f2} ($V_{1/2}$ = 75 mV, q = 1.8 e_0) for a total of 2.9 e_0.

Blocking the final transition affects, as expected, the behavior of the charge movement in the intermediate transitions of the NC-L2C channel. Because of the forward (rightward) bias of the last transition, it provides a sucking action that pulls channels to the right in the gating scheme. This sucking action does not occur when the last transition is blocked by 4AP. This can be seen by comparing curves Q_f (defined above) and Q_1–Q_3 (total gating charge − gating charge in the early steps). The sucking action is present in Q_1–Q_3 (no 4AP) and absent in Q_f, which thus lies to the right of Q_1–Q_3 in Fig. 6 *D*. The difference between Q_1–Q_3 and Q_f is maximal in the range 50–70 mV, which is the voltage range where the L2C channels open, as can be seen from the g-V curve (Fig. 6 *D*). The g-V curve parallels Q_{final} in these conditions. Interestingly, because of the sucking action, the g-V crosses Q_f (where suction is blocked by 4AP) and rises to saturation at less positive potentials than Q_f.

DISCUSSION

In this paper we have examined the mechanism of 4AP action and used it to characterize the late steps in the gating of the *Shaker* K channel. The primary goal was to isolate the intermediate steps that immediately precede the final opening transition. The experimental strategy was to use the L2C mutation to separate the late transitions from the early ones (Schoppa et al., 1992) and the potassium channel blocker 4AP (McCormack et al., 1994) to block the final opening transition. The intermediate steps are shown to consist of two transitions that carry about a quarter of the total gating charge. Our experimental approach and analysis of the data are heavily influenced by previous efforts to characterize the activation gating transitions of *Shaker* K channel (Hoshi et al., 1994; Zagotta et al., 1994a,b; Bezanilla et al., 1994) and are in good general agreement with the model of Schoppa and Sigworth (1998c). By using 4AP and demonstrating its role as a selective blocker of the final transition we were able to isolate and characterize the transitions, which immediately precede gate opening.

4AP alters the equilibrium of the final transition

The following evidence suggests that the main action of 4AP is a selective and strong effect on the final transition, which it biases toward the closed state. This effect is exerted only when 4AP occupies the channel (see Armstrong and Loboda, 2001, in this issue). 1) Normally, gating charge return is strongly retarded when channels enter the fully activated state, producing the pronounced rising phase in the tails seen in traces 3 and 4 of Fig. 1 *A*. 4AP removes this retardation, presumably by making it impossible for the channels to reach the fully activated state, as seen in Fig. 1 *B* and Fig. 4, *B* and *D*. 2) In preventing the retardation, 4AP reduces the total gating charge movement by only 5%, strongly suggesting that it affects only one transition. Clearly, the affected transition must be the final one. 3) 4AP affects neither the kinetics nor the gating charge associated with the early steps (best seen in Fig. 2). The changes in Q-V curves associated with 4AP can be attributed to the removal of the sucking action of the forward-biased final transition.

To demonstrate quantitatively that these ideas are appropriate, we developed a gating scheme somewhat similar to the Schoppa and Sigworth model. The main difference is that the early steps in the scheme have been simplified, because our main purpose was to examine the later steps. The model thus contains three early transitions, two intermediate transitions (the justification for two intermediate transitions is given below) with rates and voltage dependencies obtained in this paper, and a forward (rightward) biased final transition (cf. Schoppa and Sigworth, 1998c; Hoshi et al., 1994; Zagotta et al., 1994a,b). The differences in gating between NC and NC-L2C are accounted for by shifting the late steps to more depolarized potentials as given in the following gating schemes:

$$\begin{array}{ccccccccccccccc} & 5000 & & 7000 & & 6000 & & 4000 & & 5000 & & 6000 & & 7000 & \\ & (0.2) & & (0.4) & & (0.4) & & (0.5) & & (0.4) & & (1.1) & & (0.18) & \\ C_0 & \leftrightarrow & C_1 & \leftrightarrow & C_2 & \leftrightarrow & C_3 & \leftrightarrow & C_4 & \leftrightarrow & C_5 & \leftrightarrow & C_6 & \leftrightarrow & O \\ & (-0.4) & & (-0.6) & & (-0.6) & & (-0.6) & & (-0.5) & & (-0.7) & & (-0.52) & \\ & 600 & & 800 & & 1200 & & 1200 & & 2000 & & 600 & & 150 & \\ & \underbrace{\qquad\qquad\qquad\qquad\qquad\qquad\qquad\qquad} & & & & & & & & \underbrace{\qquad\qquad\qquad} & & & & \uparrow & \\ & \text{early steps} & & & & & & & & \text{intermediate} & & & & \text{final} & \end{array} \quad \text{(Scheme 1 (NC))}$$

$$\begin{array}{ccccccccccccccc} & 5000 & & 7000 & & 6000 & & 4000 & & 1800 & & 300 & & 800 & \\ & (0.2) & & (0.4) & & (0.4) & & (0.5) & & (0.4) & & (1.1) & & (0.18) & \\ C_0 & \leftrightarrow & C_1 & \leftrightarrow & C_2 & \leftrightarrow & C_3 & \leftrightarrow & C_4 & \leftrightarrow & C_5 & \leftrightarrow & C_6 & \leftrightarrow & O \\ & (-0.4) & & (-0.6) & & (-0.6) & & (-0.6) & & (-0.5) & & (-0.7) & & (-0.52) & \\ & 300 & & 600 & & 900 & & 1200 & & 6000 & & 10000 & & 1000 & \end{array} \quad \text{(Scheme 2 (NC+L2C))}$$

The top and bottom rows of numbers show the rates of the transitions at 0 mV. Forward rates are above each transition and backward rates are below. The numbers in parentheses show the amount of charge associated with the forward and backward rate of each transition.

Scheme 1 accounts well for the properties of NC channel gating (Fig. 7, *A* and *B*), as can be seen by comparing the simulations with the experimental records in Fig. 1, *A* and *B*. 4AP makes a dramatic gating change in NC channel gating: the rising phase in the tails (Fig. 1, *A* and *B*) is abolished. This effect is well simulated by blocking the final transition in Scheme 1 (Fig. 7, *A* and *B*). Block prevents the channels from reaching state O, from which return on repolarization is slow (rate constant 150 s^{-1} at 0 mV). Note that the final transition in the model contains only 5% of the total gating charge, consistent with the ideas expressed above.

The final transition also plays an important role as the channels are activating: the forward bias of the final transition (i.e., the equilibrium favors the open state) is responsible for sucking channels into the open state at depolarizations around −40 mV, producing the slow component in I_g ON. Block of the final transition also explains the effect of 4AP on the *Q-V* curve (Fig. 2). As seen in Fig. 2 *B*, the difference between the *Q-V* curve with and without 4AP is largest near −40 mV, the voltage where the sucking action of the final transition is maximal. The gating charge assigned to the final transition is ~5% of the total, as measured from the gating charge blocked at voltages above 0 mV (Fig. 2); above 0 mV all the channels are driven to C6 (the rightmost closed state), and only the final step is missing, blocked by 4AP.

The final transition in the NC-L2C channel is shifted to more depolarized potentials because its forward rate constant is slower and its backward rate constant faster. The faster backward rate (1000 s^{-1} rather than 150 s^{-1} at 0 mV) also explains the absence of the rising phase in the tail even without 4AP. Nonetheless, block of the final transition with 4AP has a detectable effect (Fig. 1, *C* and *D*, and Fig. 7, *C* and *D*) that is well simulated by abolishing the final transition. 4AP blocks 5% of the total gating charge in NC-L2C as well as in NC (Fig. 2, *A* and *B*), which corresponds to the amount of charge in the final transition.

In summary, we believe that the main action exerted by 4AP when it occupies a channel is to reverse-bias the final transition, forcing the gate to close with 4AP inside the channel (see Armstrong and Loboda, 2001, this issue).

The L2C mutation reveals the intermediate steps in the activation sequence

When the final transition is blocked by 4AP, the first event on repolarization after a large step is the leftward movement of channels from C6 into and through the intermediate states. This is followed by the early transitions (see diagram above). Multiple components are hard to distinguish in NC channel tails because the intermediate and early transitions have similar kinetics. The NC-L2C channel, on the other hand, has two easily resolved kinetic components (Fig. 3 *B*), consistent with the conclusion of Schoppa and Sigworth (1998c) that the L2C mutation speeds up the backward rates of the intermediate transitions. This makes them distinguishable from the early steps, which generate the slow component in the tail gating currents. Thus, using L2C and confining V_m to the range from 0 to +100 mV allows us to study the intermediate transitions, uncontaminated by the early ones that do not occur in this voltage range. Further, addition of 4AP eliminates the last transition, leaving only the intermediate transitions. Scheme 2, which has two intermediate transitions, simulates well the time course of the fast component after depolarizations of different durations (see Fig. 8, which mimics the records in Fig. 4). Without 4AP the fast component is seen only transiently; its amplitude decreases as channels enter state O (Fig. 3, *A* and *C*, and Fig. 8 *A*). This introduces a slow transition, O to C_6, on repolarization, thus eliminating the fast component. Interestingly, the envelope of the decay of fast-component am-

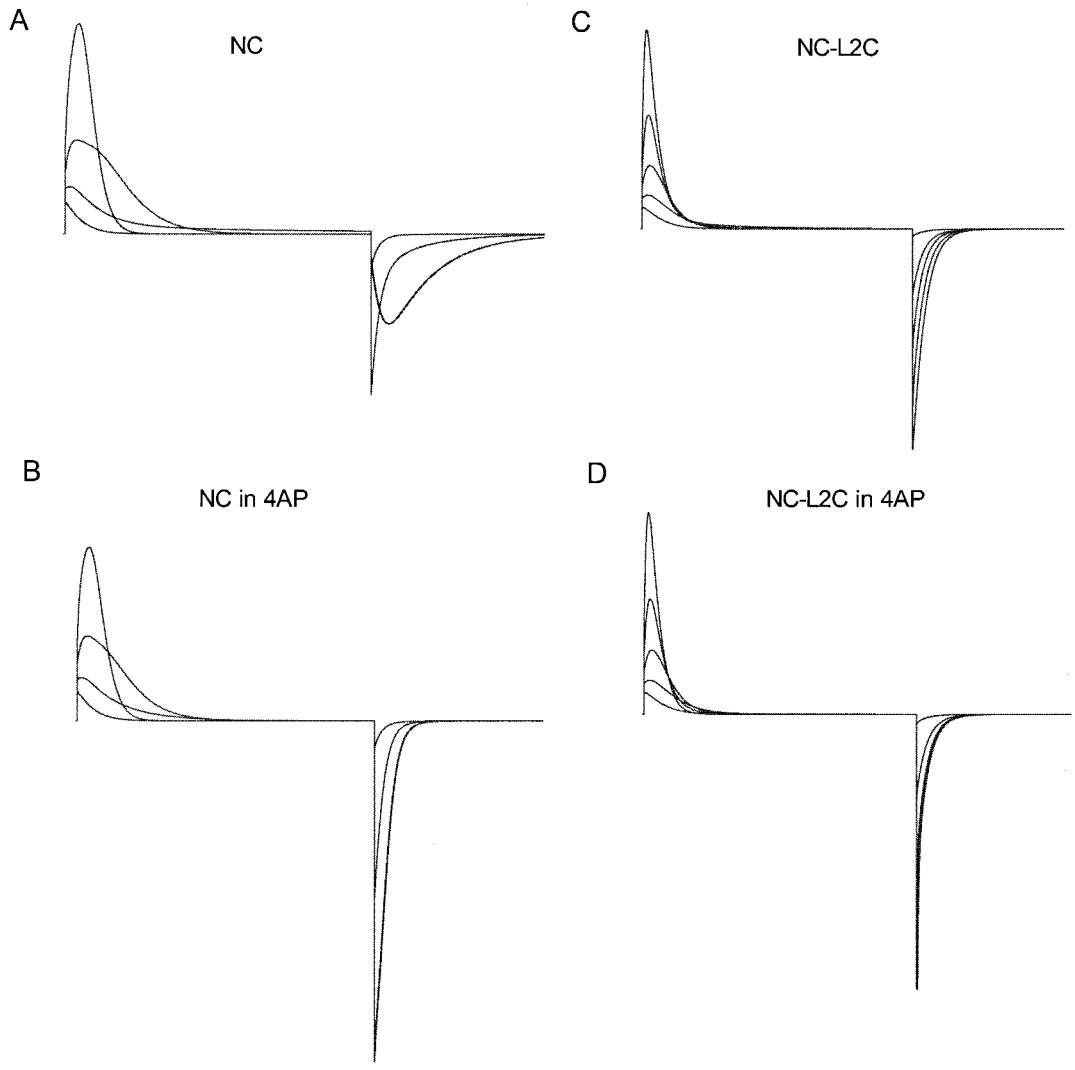

FIGURE 7 Gating current simulations of the NC (Scheme 1) and NC-L2C (Scheme 2) channels. The simulations use the same protocols as in Fig. 1 and closely resemble the gating current records shown in that figure. The effect of 4AP on the gating currents was well simulated by blocking the final transition (compare Fig. 1, *B* and *D*, with Fig. 7, *B* and *D*).

plitudes (caused by entry into state O; Fig. 4, *A* and *C*) is the same in conducting and nonconducting channels, which suggests that the nonconducting channel also undergoes a gate-opening transition with about the same rate as the conducting channel. When 4AP is added the final transition is blocked, so the channels remain in C6 after a large depolarization, never entering state O and thus never experiencing the slow return from this state on repolarization. The result is that the fast component remains large (compare Fig. 4, *B* and *D*, and Fig. 8 *B*).

The fast component carries about a quarter of the total gating charge (Fig. 6), or 2.9 e_0 if the total gating charge is 13 e_0 (reference). A single transition with 2.9 e_0 cannot account for the *Q-V* and kinetics of the gating charge in the fast component (see Fig. 6 *C*). Kinetics and voltage dependence of the fast gating current component are well fitted with two sequential concerted steps carrying 1.1 and 1.8 e_0 respectively (Fig. 5, *C* and *D*).

This paper provides clear evidence that 4AP reverse-biases or abolishes the final opening transition without affecting other transitions. Based on this observation we used the model developed in this paper for the NC channel to reexamine the literature concerning 4AP action on conducting channels. The behavior of conducting channels can be explained in detail by this model, as shown in the next paper.

REFERENCES

Aggarwal, S. K., and R. MacKinnon. 1996. Contribution of the S4 segment to gating charge in the *Shaker* K^+ channel. *Neuron.* 16:1169–1177.

Armstrong, C. M., and F. Bezanilla. 1973. Currents related to the movement of the gating particles of the sodium channels. *Nature.* 242: 459–461.

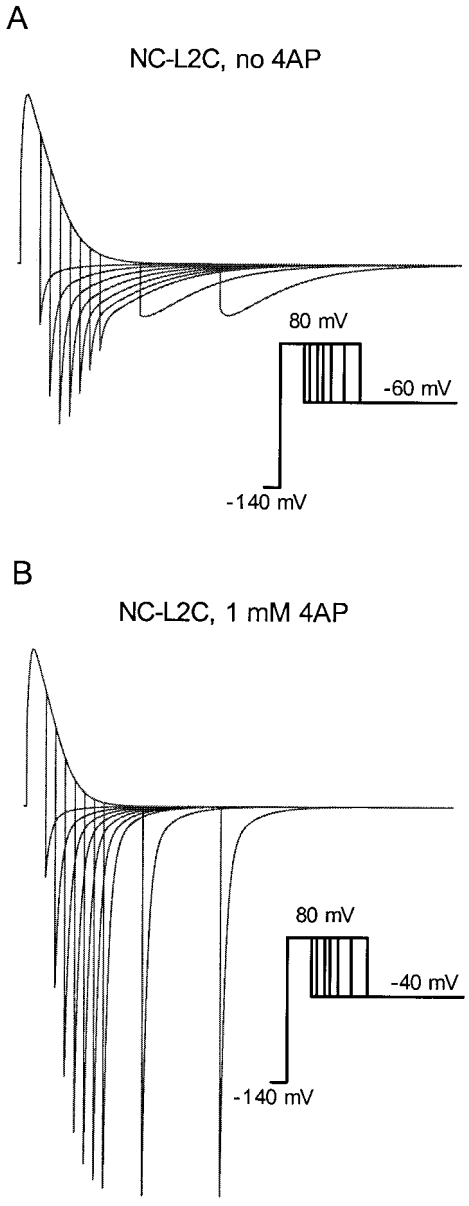

FIGURE 8 Simulations using Scheme 2 show why the fast component in the tails of the NC-L2C channel are large and persistent when 4AP blocks the final transition. (*A*) Simulations with Scheme 2 using the voltage protocol of Fig. 4. The amplitude of the fast component decreases with increased duration of the pulse as channels enter the fully activated state from which return is slow. (*B*) The same voltage protocol as in *A* was used. Simulated block of the final transition in Scheme 2 leads to a dramatic increase in the size of the fast component, analogous to the effect of 4AP in Fig. 4.

Armstrong, C. M., and A. Loboda. 2001. Model for 4-aminopyridine action on K channels: similarities to tetraethylammonium ion action. *Biophys. J.* 81:895–904.

Bezanilla, F., E. Perozo, D. M. Papazian, and E. Stefani. 1991. Molecular basis of gating charge immobilization in *Shaker* potassium channels. *Science.* 254:679–683.

Bezanilla, F., E. Perozo, and E. Stefani. 1994. Gating of *Shaker* K^+ channels. II. The components of gating currents and a model of channel activation. *Biophys. J.* 66:1011–1021.

Holmgren, M., M. E. Jurman, and G. Yellen. 1996. N-type inactivation and the S4–S5 region of the *Shaker* K^+ channel. *J. Gen. Physiol.* 108: 195–206.

Hoshi, T., W. N. Zagotta, and R. W. Aldrich. 1990. Biophysical and molecular mechanisms of *Shaker* potassium channel inactivation. *Science.* 250:533–538.

Hoshi, T., W. N. Zagotta, and R. W. Aldrich. 1994. *Shaker* potassium channel gating. I. Transitions near the open state. *J. Gen. Physiol.* 103:249–278.

Jurman, M. E., L. M. Boland, L. Y. Liu, and G. Yellen. 1994. Visual identification of individual transfected cells for electrophysiology using antibody-coated beads. *BioTechniques.* 17:876–881.

Kirsch, G., J. Z. Yeh, and G. S. Oxford. 1986. Modulation of aminopyridine block of potassium currents in squid axon. *Biophys. J.* 50:637–644.

Ledwell, J. L., and R. W. Aldrich. 1999. Mutations in the S4 region isolate the final voltage-dependent cooperative step in potassium channel activation. *J. Gen. Physiol.* 113:389–414.

MacKinnon, R. 1991. Determination of the subunit stoichiometry of a voltage-activated potassium channel. *Nature.* 350:232–235.

McCormack, K., W. J. Joiner, and S. H. Heinemann. 1994. A characterization of the activating structural rearrangements in voltage-dependent *Shaker* K^+ channels. *Neuron.* 12:301–315.

Melishchuk, A., A. Loboda, and C. Armstrong. 1998. Loss of *Shaker* K channel conductance in 0 K^+ solutions: role of the voltage sensor. *Biophys. J.* 75:1828–1835.

Perozo, E., R. MacKinnon, F. Bezanilla, and E. Stefani. 1993. Gating currents from a nonconducting mutant reveal open-closed conformations in *Shaker* K^+ channels. *Neuron.* 11:353–358.

Schoppa, N. E., K. McCormack, M. A. Tanouye, and F. J. Sigworth. 1992. The size of gating charge in wild-type and mutant *Shaker* potassium channels. *Science.* 255:1712–1715.

Schoppa, N. E., and F. J. Sigworth. 1998a. Activation of *Shaker* potassium channels. I. Characterization of voltage-dependent transitions. *J. Gen. Physiol.* 111:271–294.

Schoppa, N. E., and F. J. Sigworth. 1998b. Activation of *Shaker* potassium channels. II. Kinetics of the V2 mutant channel. *J. Gen. Physiol.* 111: 295–311.

Schoppa, N. E., and F. J. Sigworth. 1998c. Activation of *Shaker* potassium channels. III. An activation gating model for wild-type and V2 mutant channels. *J. Gen. Physiol.* 111:313–342.

Seoh, S. A., D. Sigg, D. M. Papazian, and F. Bezanilla. 1996. Voltage sensing residues in the S2 and S4 segments of *Shaker* K^+ channel. *Neuron.* 16:1159–1167.

Stefani, E. L. Toro, E. Perozo, and F. Bezanilla. 1994. Gating of *Shaker* K^+ channels. I. Ionic and gating currents. *Biophys. J.* 66:996–1010.

Stühmer, W., F. Conti, M. Stocker, O. Pongs, and S. H. Heinemann. 1991. Gating currents of inactivating and non-inactivating potassium channels expressed in *Xenopus* oocytes. *Pflügers Arch. Eur. J. Physiol.* 418: 423–429.

Tempel, B. L., D. M. Papazian, T. L. Schwarz, Y. N. Jan, and L. Y. Jan. 1987. Sequence of a probable potassium channel component encoded at the *Shaker* locus of *Drosophila*. *Science.* 237:770–775.

Tytgat, J., and P. Hess. 1992. Evidence for cooperative interactions in potassium channel gating. *Nature.* 352:800–803.

Zagotta, W. N., T. Hoshi, J. Dittman, and R. W. Aldrich. 1994a. *Shaker* potassium channel gating. II. Transitions in the activation pathway. *J. Gen. Physiol.* 103:279–319.

Zagotta, W. N., T. Hoshi, and R. W. Aldrich. 1994b. *Shaker* potassium channel gating. III. Evaluation of kinetic models for activation. *J. Gen. Physiol.* 103:321–362.